PCCP

PAPER

View Article Online
View Journal | View Issue

Cite this: *Phys. Chem. Chem. Phys.*, 2018, **20**, 4893

A dynamical process of optically trapped singlet ground state $^{85}Rb^{133}Cs$ molecules produced *via* short-range photoassociation

Zhonghao Li,[ab] Ting Gong,[ab] Zhonghua Ji,[ab] Yanting Zhao,*[ab] Liantuan Xiao[ab] and Suotang Jia[ab]

Received 17th November 2017,
Accepted 17th January 2018

DOI: 10.1039/c7cp07756d

rsc.li/pccp

We investigate the dynamical process of optically trapped $X^1\Sigma^+$ ($v'' = 0$) state $^{85}Rb^{133}Cs$ molecules distributed in $J'' = 1$ and $J'' = 3$ rotational states. The considered molecules, formed from short-range photoassociation of mixed cold atoms, are subsequently confined in a crossed optical dipole trap. Based on a phenomenological rate equation, we provide a detailed study of the dynamics of $^{85}Rb^{133}Cs$ molecules during the loading and holding processes. The inelastic collisions of $^{85}Rb^{133}Cs$ molecules in the $X^1\Sigma^+$ ($v'' = 0$, $J'' = 1$ and $J'' = 3$) states with ultracold ^{85}Rb (or ^{133}Cs) atoms are measured to be 1.0 (2) $\times$ 10^{-10} cm^3 s^{-1} (1.2 (3) $\times$ 10^{-10} cm^3 s^{-1}). Our work provides a simple and generic procedure for studying the dynamical process of trapped cold molecules in the singlet ground states.

Introduction

The preparation and manipulation of ultracold molecules have attracted significant interest in the past few years. Due to strong dipole–dipole interactions, ultracold heteronuclear molecules in the absolute ground state are particularly attractive: with permanent electric dipole moments (EDMs) ranging from a half to several Debye,[1] such molecules could interact strongly with external fields, as well as with each other *via* long-range dipole–dipole forces. These novel molecular properties promise interesting applications in precision measurement,[2–4] quantum control of cold chemical reactions,[5,6] and quantum computation.[7]

At present, there exist various proposals on the preparation of ground-state polar molecules, in particular those in the lowest rovibrational ground state. In this context, one of the most promising approaches involves the combination of magnetoassociation (MA) with stimulated Raman adiabatic passage (STIRAP), in sense of achievable temperature and phase space density. This has led to the achievement of $^{40}K^{87}Rb$,[8] $^{87}Rb^{133}Cs$,[9,10] $^{23}Na^{40}K$[11] and $^{23}Na^{87}Rb$.[12] However, this scheme is only suitable for atomic species where the MA is available and requires the initial cold atomic state to be nearly degenerate. Alternatively, photoassociation (PA) as a simple and universal method has been extensively applied. For example, the combination of PA with "pump–dump" has been applied to $^{85}Rb^{133}Cs$.[13] Nevertheless, the transfer efficiency is low due to the large branching ratio to other electronic states and complicated optical pathways. The PA has also been combined with STIRAP in $^{41}K^{87}Rb$.[14] While this gives rise to a transfer process that is highly efficient and state-selective, the ground-state molecules can only be formed once per experimental cycle, thus limiting the accumulation of molecules. A third approach uses direct short-range PA, where the direct spontaneous emission after PA allows creation of molecules in the singlet ground state. Such a scheme has been successfully implemented in $^{39}K^{85}Rb$,[15] $^{23}Na^{133}Cs$,[16] $^{7}Li^{133}Cs$,[17] $^{85}Rb^{133}Cs$[18], $^{7}Li^{85}Rb$[19] *etc*. Remarkably, the continuous production and simultaneous trapping of molecules *via* this method has promising potential to produce a large number of molecules in special molecular states *via* optical pumping, such as vibrational cooling[20] and rotational cooling.[21] These samples provide the basis to form pair-supersolid phases[22] and molecular Bose–Einstein condensates.[23,24]

In addition, there have been significant efforts in confining molecules using various types of traps, such as the electrostatic trap,[25] magnetic trap,[26] and optical dipole trap (ODT),[27] or their combinations. The former two traps only apply for particular molecules, such as the electrostatic trap for polar molecules and the magnetic trap for paramagnetic molecules in the low-field-seeking states. By contrast, the ODT is more widely used. The formation of molecules *via* PA and confinement in an ODT has been demonstrated. For example, the quasi-electrostatic trap (QUEST) has been used to confine $^{133}Cs_2$,[28,29] $^{87}Rb_2$,[30]

[a] *Shanxi University, State Key Laboratory of Quantum Optics and Quantum Optics Devices, Institute of Laser Spectroscopy, Wucheng Rd. 92, 030006 Taiyuan, China. E-mail: zhaoyt@sxu.edu.cn*
[b] *Shanxi University, Collaborative Innovation Center of Extreme Optics, Wucheng Rd. 92, 030006 Taiyuan, China*

$^{85}Rb^{133}Cs$,[31] and $^{7}Li^{133}Cs$,[32,33] while the far off-resonance optical dipole trap (FORT) has been applied to confine $^{87}Rb_2$ and $^{85}Rb_2$.[34,35] These trapped samples have been used for the calculation of the atom–molecule inelastic collision rate coefficients,[28,29,32,33] verification of the data acquisition technique,[34] and determination of the molecule number.[35] Motivated by the significant interest in the lowest vibrational $X^1\Sigma^+$ ($v'' = 0$) state, it is desirable to seek an effective production and storage of these ground state molecules. Unlike the above trapped molecular samples which are either in the $a^3\Sigma^+$ states or high-lying levels of $X^1\Sigma^+$ states, in this work we aim at the creation and confinement of molecules in the $X^1\Sigma^+$ ($v'' = 0$) state.

For $^{85}Rb^{133}Cs$ molecules, the detailed information of the $2^1\Pi_1$, $2^3\Pi_{0^-}$, $2^3\Pi_{0^+}$, $2^3\Pi_1$, $3^3\Sigma_1^+$ excited states *via* short-range PA have been reported,[37–40] which give abundant choices with an effectively intermediate state for the preparation of $X^1\Sigma^+$ ($v'' = 0$) state molecules. Specially, C. D. Bruzewicz and co-workers have studied the continuous formation of ultracold $^{85}Rb^{133}Cs$ molecules in $X^1\Sigma^+$ ($v'' = 0$–10) *via* short-range PA to the $2^3\Pi_{0^+}$ ($v = 10$) intermediate state.[18] These results provide a powerful basis for the realization of optical trapping of $X^1\Sigma^+$ ($v'' = 0$) state molecules *via* short-range PA. Although these molecules in the $X^1\Sigma^+$ ($v'' = 0$) state have been produced *via* short-range PA, experimental achievement of the optical trapping has not yet been reported so far.

In this paper, ultracold $^{85}Rb^{133}Cs$ molecules in the lowest vibrational ground state are confined in a crossed ODT. The ground state molecules are prepared *via* short-range PA and measured selectively through the sensitive photoionization (PI) detection technology. A phenomenological rate equation is introduced to achieve the quantitative analysis of the loading and holding procedures of the $X^1\Sigma^+$ ($v'' = 0$) state (to be precise, the $J'' = 1$ and $J'' = 3$ states of $X^1\Sigma^+$ ($v'' = 0$)) molecules in ODT. It is found that the inelastic molecular collision and the vibrational redistribution are negligible. In addition, the inelastic collisions of $^{85}Rb^{133}Cs$ molecules in the $X^1\Sigma^+$ ($v'' = 0, J'' = 1$ and $J'' = 3$) states with ultracold ^{85}Rb (or ^{133}Cs) atoms are measured.

Experimental setup

Fig. 1(a) shows a diagram illustrating the formation and detection mechanism of ultracold $^{85}Rb^{133}Cs$ molecules in the lowest vibrational ground state. (i) PA. Pairs of colliding ^{85}Rb and ^{133}Cs atoms are excited to a deeply bound state in a short range. (ii) Decay. After the two-photon-cascade spontaneous emission process,[41] the stable state molecules are distributed in different vibrational states.[18] (iii) Detection. The molecules are detected using the PI technology.

As shown in Fig. 1(b), the ultracold ^{85}Rb and ^{133}Cs atoms are initially cooled and trapped in overlapped dual species magneto-optical traps (MOTs). The MOTs are operated in the dark spontaneous force optical traps (dark-SPOTs) configuration, which provides the atomic sample with a high atomic density and a low collision rate.[42] The vacuum background pressure in the chamber is kept at about 3×10^{-7} Pa. A pair of anti-Helmholtz coils generates a magnetic gradient of about 15 G cm^{-1}. Four Littrow external-cavity diode lasers (Toptica, DL100) locked *via* a saturation absorption spectroscopy technique provide the trapping and repumping beams for ^{85}Rb and ^{133}Cs. All of these beams are 15 mm in diameter. The total power of the trapping laser is around 36 mW, and the total power of the repumping laser is around 8 mW, respectively. The dark-SPOTs are achieved by filling the depumping beams in the dark region of the repumping beams. The dark region is created by a black dot in the center of the mixed repumping beams. Both depumping beams have a power of about 80 μW with 3 mm diameter. The overlap of atomic clouds is verified using two charge-coupled device (CCD) cameras placed along the horizontal and vertical directions, respectively. In this way, about 1×10^7 of ^{85}Rb atoms are formed in the $5S_{1/2}$ ($F = 2$) state with a density of 8×10^{10} cm^{-3}, and about 2×10^7 ^{133}Cs atoms are formed in the $6S_{1/2}$ ($F = 3$) state with a density of 1.5×10^{11} cm^{-3}.

The PA process is achieved by employing a tunable Ti:sapphire laser system (M Squared, Sols Ti:sapphire) with a typical linewidth of 100 kHz and an output power of up to 1.5 W. We focus the PA beam on the center of the overlapped dark-SPOTs with the Gaussian radius of 150 μm. The PA laser is locked *via* the transfer cavity technique based on an ultrastable He–Ne laser as a reference laser. The produced molecules will subsequently decay to the ground state. The frequency is monitored using a commercial wavelength meter (High Finesse-Angstrom, WS-7R) with an absolute accuracy of 0.002 cm^{-1} (about 60 MHz), which is calibrated with the Rb atomic transition line.

The PI laser pathways as shown in Fig. 1(a) are chosen to observe the produced ground state molecules. The PI laser is a tunable dye laser (CBR-G-18EG, Spectra physics, wavelength is about 651.8 nm, pulse duration of 7 ns, diameter is about 3 mm, pulse energy is about 1 mJ, and repetition rate of 10 Hz). The dye laser is pumped by the second harmonic of an Nd-YAG laser (Spectra physics, INDIE-40-10-HG, wavelength of 532 nm) and operated on DCM dissolved in dimethyl sulfoxide (DMSO). The ions formed in this process are accelerated by a pulsed electric field with a duration time of 20 μs. After the acceleration procedure, these moving ions will fly freely with a length of 68 mm. Finally, the ions are detected using a pair of microchannel plates (MCPs). The electric signals are detected, amplified, monitored on a digital oscilloscope, and recorded using an NI PCI-1714 card following a boxcar (Boxcar, SRS-250) with 10 averages.

An ODT is built to trap the formed molecules. The simplest configuration of ODT is a single focused beam, which creates a highly anisotropic trap with relatively weak confinement along the propagation axis and tight confinement in the perpendicular direction. By crossing two focused beams, one can create a nearly isotropic and tight confinement in all dimensions, allowing formation of denser samples. In our experiment, the ODT is realized with a linearly polarized broadband fiber laser (IPG Photonics, YLR-300-AC) with a central wavelength of 1070 nm and a linewidth of 2 nm. The IPG laser is divided

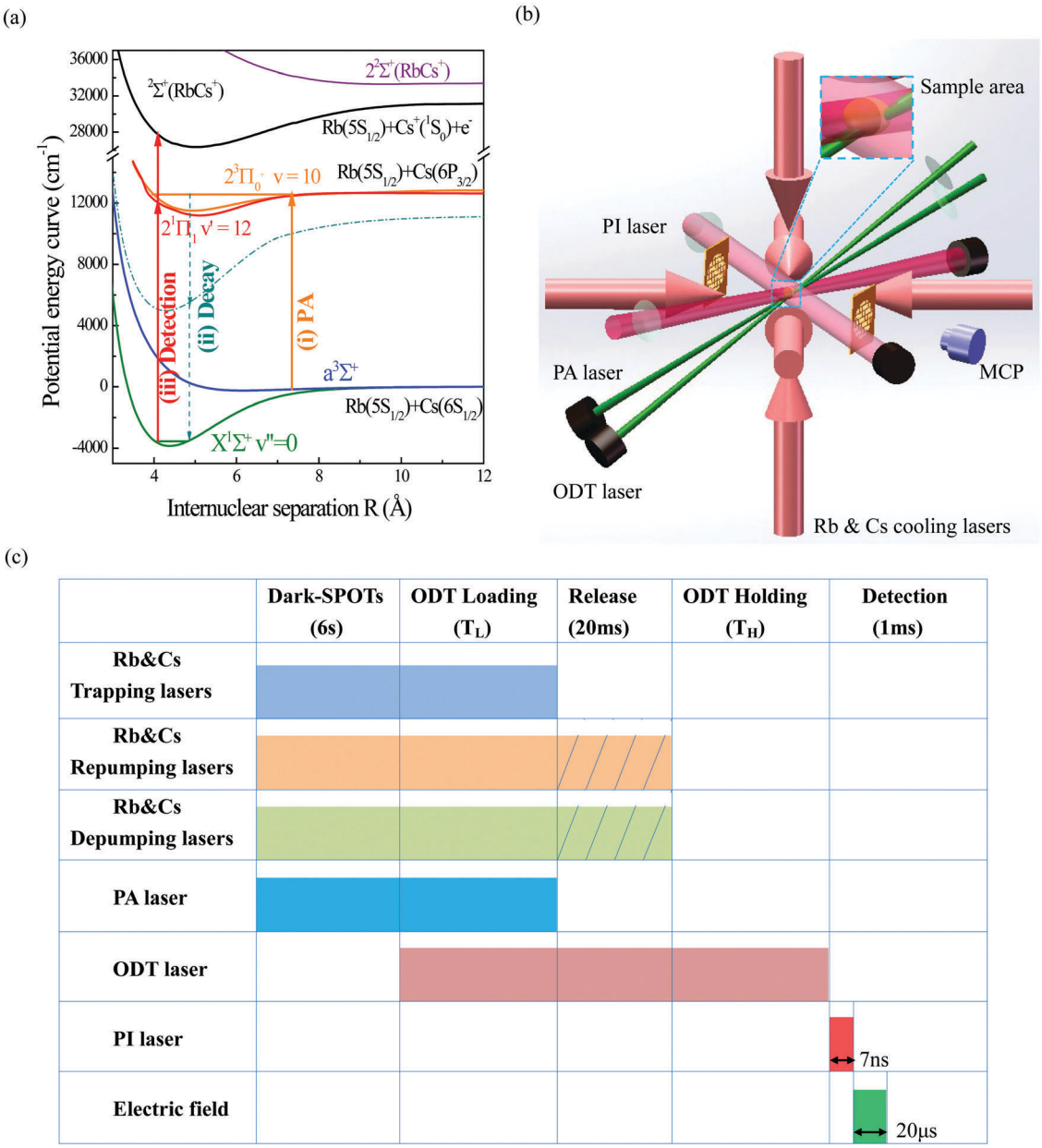

Fig. 1 (a) Formation and detection mechanism for ultracold $^{85}Rb^{133}Cs$ molecules in the $X^1\Sigma^+$ ($v'' = 0$) state. The potential energy curves are based on the data in ref. 36. The related pathways are the same as ref. 18. (b) A brief diagram of optical elements near the vacuum chamber. (c) Experimental time sequence. The shadow with different colors means "on", the blank means "off", and the rectangle with lines means "selectively on or off". The lasers are kept on in order to push the co-trapped cold atoms out of the ODT, while the lasers are turned off in order to keep the trapped cold atoms in the ODT.

into two beams with orthogonal linear polarization. As shown in Fig. 1(b), two ODT beams are crossed on the center of the dark-SPOTs with an angle of 45°. The waists of these two beams are both 76 (2) μm. The frequencies are shifted oppositely by 110 MHz by using two acousto-optic modulators (AOMs) to prevent DC interference effects and allow rapid control of the ODT ($\tau < 1$ μs). The AC Stark shift produces a conservative potential with a minimum at the focus, where the ultracold atomic and molecular sample can be trapped. We find that it is advantageous to move the point of the crossed ODT below the center of dark-SPOTs by 0.5 mm along the direction of gravity. The total power of ODT beams is normally around 5 W. About 8×10^5 of ^{85}Rb atoms at the $5S_{1/2}$ ($F = 2$) state with a density of 2×10^{11} cm^{-3} and about 1.5×10^6 ^{133}Cs atoms at the $6S_{1/2}$ ($F = 3$) state with a density of 4×10^{11} cm^{-3} are transferred from the dark-SPOTs.

The time sequence of the experiment is shown in Fig. 1(c), which is divided into five stages. (1) The loading procedure of dark-SPOTs. The PA procedure occurs simultaneously and the duration time is about 6 s. All the dark-SPOTs lasers are turned on in the presence of a magnetic field to trap cold atoms. The cooling and repumping lasers are chosen at the optimized

value for the largest loading rate. (2) The loading procedure of ODT. (3) The expansion procedure of untrapped atoms and molecules with a duration time of 20 ms. In this procedure, the depumping and repumping lasers can be selected to keep on as the pushing lasers to remove the mixed atoms in ODT or are turned off for the investigation of atom–molecule collisions. (4) The holding procedure of trapped samples in ODT. In this period, only the dipole laser is kept on. (5) Detection. The trapped molecules are detected *via* PI through resonance-enhanced two-photon ionization (RETPI).

Experimental results and analysis

Optical trapping of $X^1\Sigma^+$ ($v'' = 0$) state molecules distributed in $J'' = 1$ and $J'' = 3$ rotational states

Fig. 2(a) shows the rotational structure of the excited $2^3\Pi_{0^+}$ ($v = 10$) state, which agrees with the measured results in ref. 18. Because this state has large free-to-bound and bound-to-bound Franck–Condon factors (FCFs), it can be used for the preparation of molecules in the $X^1\Sigma^+$ ($v'' = 0$) state with the ratio of about 30% efficiently. In the following experiments, the frequency of the PA laser is fixed at $J = 1$. The rotational distributions of molecules in the $X^1\Sigma^+$ ($v'' = 0$) state are $J'' = 1$ and $J'' = 3$ according to ref. 41 and also have been confirmed in our measurement using depletion spectroscopy. To be concise, $X^1\Sigma^+$ ($v'' = 0$) represents the $X^1\Sigma^+$ ($v'' = 0$, $J'' = 1$ and $J'' = 3$) states in the following contexts.

The $X^1\Sigma^+$ ($v'' = 0$) state molecules could be state-selectively detected *via* RETPI. The PI spectra have been measured using the scanning PI laser (frequency of about 630–680 nm) while keeping the PA laser fixed at the $2^3\Pi_{0^+}$ ($v = 10, J = 1$) level. Here we show a part of PI spectra of the $X^1\Sigma^+$ ($v'' = 0$) state in Fig. 2(b). Since the frequency bandwidth of the PI laser (about 0.2 cm^{-1}) is larger than the energy spacing of the rotational level, it is impossible to distinguish rotational levels. The spectra allow for straightforward assignment of the observed transitions between vibrational states based on ref. 18 and 43. We assign the $\sim$15278.31 cm^{-1} peak to the $2^1\Pi_1$ ($v' = 10$) $\leftarrow$ $X^1\Sigma^+$ ($v'' = 0$) transition and the $\sim$15341.41 cm^{-1} peak to the $2^1\Pi_1$ ($v' = 12$) $\leftarrow$ $X^1\Sigma^+$ ($v'' = 0$) transition. The red line is the Lorentzian fitting. In following work, the PI laser frequency is fixed at about 15341.41 cm^{-1}.

Based on the sensitive PI technology, the molecules in the $X^1\Sigma^+$ ($v'' = 0$) state can be compared directly with the time of flight (TOF) mass spectrum under two conditions: "ODT off" and "ODT on". The "ODT off" means the molecules are released free after a regular PA procedure without ODT and then detected, while the "ODT on" means the molecules are transferred to ODT and then detected. In order to obtain obvious contrast, we record the TOF mass spectrum when the PA laser and all cooling lasers are turned off 20 ms before the detection procedure under these two conditions. With the data in Fig. 2(c), the molecular ion signal is 5 times enhanced in "ODT on" compared with that in "ODT off". These results show that the $^{85}Rb^{133}Cs$ molecules in the $X^1\Sigma^+$ ($v'' = 0$) state have been

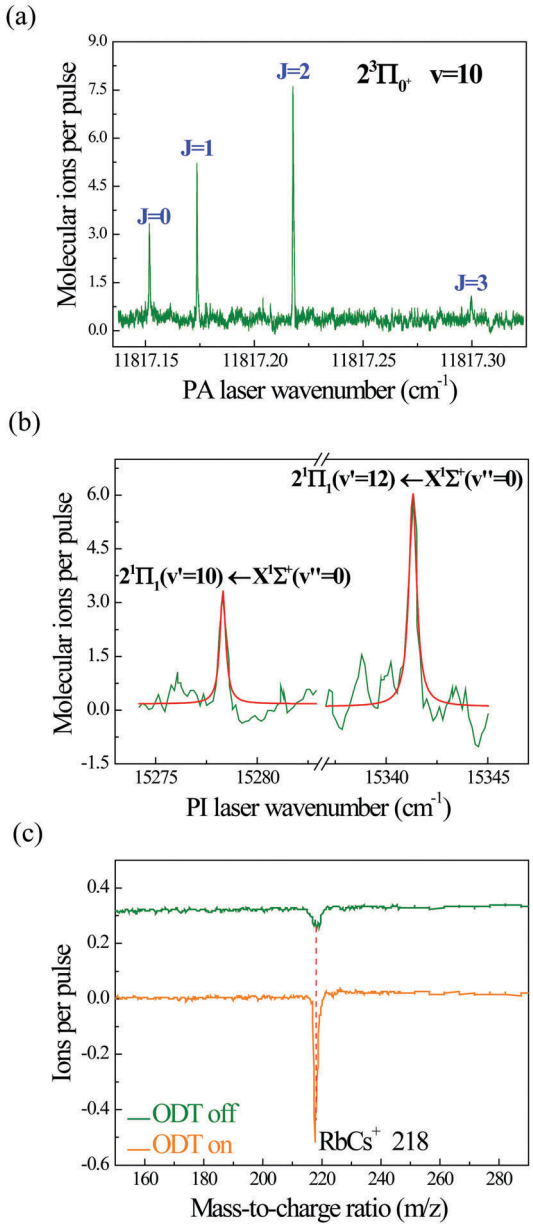

Fig. 2 (a) PA spectrum of the $2^3\Pi_{0^+}$ ($v = 10$) state, which is the intermediate state for the preparation of $^{85}Rb^{133}Cs$ molecules in the $X^1\Sigma^+$ ($v'' = 0$) state. In the following experiments, the frequency of the PA laser is fixed at $J = 1$. (b) PI spectrum of molecules in the $X^1\Sigma^+$ ($v'' = 0$) state. In the following experiments, the frequency of the PI laser is fixed at the transition of $2^1\Pi_1$ ($v' = 12$) $\leftarrow$ $X^1\Sigma^+$ ($v'' = 0$). (c) Mass spectrum under two conditions: "ODT off" and "ODT on".

trapped in the ODT. In addition, the $\Delta m/z$ value is 1.18 by fitting the data with the Lorentzian function. Considering the m/z value of $^{85}Rb^{133}Cs^+$ is 218, the resolution of the TOF mass spectrometer can be found as 185.

Loading procedure of optical trapped molecules

The dynamical processes of $^{85}Rb^{133}Cs$ molecules in the ODT will be analyzed in two different procedures: loading and holding. The loading procedure of molecules in the $X^1\Sigma^+$ ($v'' = 0$)

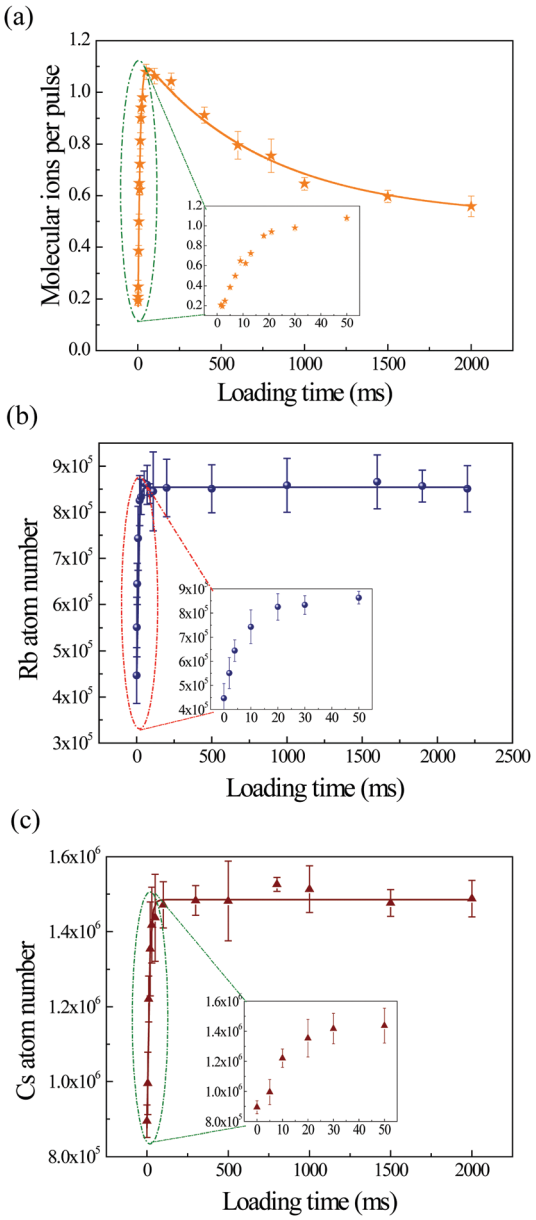

Fig. 3 ODT loading procedures of (a) ^{85}Rb^{133}Cs molecules in the $X^1\Sigma^+$ ($v'' = 0$) state, (b) ^{85}Rb atoms, and (c) ^{133}Cs atoms. All the data are recorded at holding time T_H = 1 ms. Insets: The molecule and atom numbers at the initial time.

state is observed [see Fig. 3(a)]. As we can see, the number of molecules in the $X^1\Sigma^+$ ($v'' = 0$) state loaded into the ODT increases rapidly until reaching a maximum value, which is followed by a number decrease due to a loss process.

A phenomenological rate equation is introduced to describe dynamical processes of molecules in the loading procedure.[44] The molecule number $N_{mol}(t)$ in the loading procedure can be described as

$$\frac{dN_{mol}(t)}{dt} = R_L e^{-\gamma t} - \Gamma_L N_{mol}(t) - \beta_L \int_V n^2(r,t) dr^3. \quad (1)$$

Here R_L is the maximum loading rate when the molecules are loaded into ODT at the initial time, γ represents the loss rate of molecules, Γ_L denotes the single molecular collision with both background gas and co-trapped cold samples (^{85}Rb atoms and ^{133}Cs atoms) in the dark-SPOTs, and β_L is the loss rate of molecule–molecule cold collisions. The subscript L is used to distinguish the loss rates during the loading process from the holding process in the ODT. Since the number of trapped molecules is much smaller (see the text below) than the trapped atoms, while their volumes are nearly the same,[32] the molecular density is much lower than the atomic density. Considering the universal inelastic rates for Rb–RbCs, Cs–RbCs, and RbCs–RbCs inelastic collisions are at the same order,[33] the β_L is ignorable compared to the Rb–RbCs and Cs–RbCs inelastic loss rates. Thus eqn (1) can be reduced as

$$\frac{dN_{mol}(t)}{dt} = R_L e^{-\gamma t} - \Gamma_L N_{mol}(t) \quad (2)$$

The analytical solution to this equation is

$$N_{mol}(t) = \frac{e^{-\Gamma_L t}\left(\Gamma_L N_0 - R_L + e^{(\Gamma_L - \gamma)t} R_L - N_0 \gamma\right)}{\Gamma_L - \gamma}. \quad (3)$$

Here, N_0 is the number of molecules loaded into ODT when the ODT beams are turned on. Based on this solution, it is expected that the number of molecules increases linearly with the initial loading time, $N_{mol}(t) = R_L t$. This is consistent with our observation. We choose the initial 15 ms to fit the maximum loading rate of R_L = 47 (2) s^{-1} ions per pulse while the other parameters in the loading procedure are determined by fitting the measured ion signal to eqn (3) (shown in the inset of Fig. 3(a)).

Based on eqn (3), if γ is zero, the number of molecules will gradually increase to a maximum value. The Γ_L and γ are fitted to be 75 (4) s^{-1} and 1.4 (2) s^{-1} ions per pulse with the experimental data. The presence of γ causes the decrease of the molecule number in the loading procedure. The measured number of ^{85}Rb and ^{133}Cs atoms in the PA region, respectively, is not affected by the presence of ODT, which can exclude the possibility that the loss rate is induced by the decrease of atom number in the PA region. We then measure the number of trapped Rb and Cs atoms in the ODT during the loading procedure as both atoms and molecules are loaded into the ODT simultaneously. The results are shown in Fig. 3(b) and (c). The fitting curves are also based on eqn (1), now modified for atom number N_{atom}. The number of atoms increases until reaching a maximum value. This is because the γ_{atom}, which represents the loss rate of the MOT atoms,[44] is zero for that there is no operation for dark-SPOT lasers in our experiment. We observe that the number of trapped molecules and atoms reached the maximum values at nearly the same time, although their dynamics subsequently are quite different. Thus we attribute the loss rate γ_{atom} to the loss rate of RbCs molecules in dark-SPOTs, as induced by the trapped atoms in ODT.

Holding procedure of optical trapped molecules

First, we compare the time evolution of the molecule number in "ODT off" and "ODT on". As shown in Fig. 4(a), the molecule number decreases quickly and has a shorter lifetime in "ODT off" compared to the "ODT on" case. The starting point in "ODT off" is the beginning of the release procedure and the one in

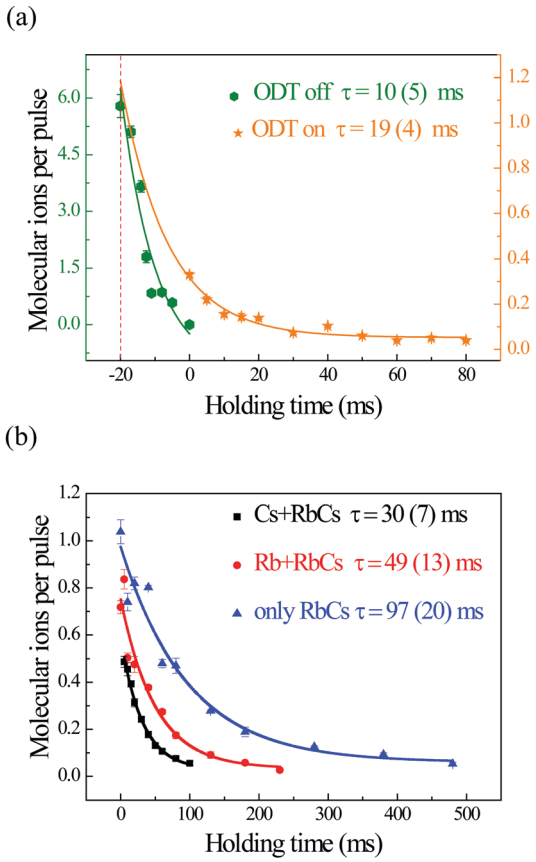

Fig. 4 Holding procedure of $^{85}Rb^{133}Cs$ molecules in the $X^1\Sigma^+$ ($v'' = 0$) state. (a) The time evolution of $X^1\Sigma^+$ ($v'' = 0$) state molecules in "ODT off" and "ODT on". (b) The time evolution of $X^1\Sigma^+$ ($v'' = 0$) state molecules in the holding procedure in the absence of co-trapped atoms, and in the presence of Rb and Cs atoms, respectively.

"ODT on" is the beginning of the ODT holding procedure. Because the untrapped samples can escape from the region of detection and almost cannot be observed after the release, the trapped sample could only be observed during the holding procedure. The trapped molecules loaded into ODT are the ones at the beginning of the release procedure and the number is fitted to be about 1.2 (1) ions per pulse (dashed line shown in Fig. 4(a)) according to the measurement of "ODT on". Considering that the initial number in dark-SPOTs is about 6.0 (5) ions per pulse, the transfer efficiency of the $X^1\Sigma^+$ ($v'' = 0$) state molecules from dark-SPOTs to ODT is estimated to be 20 (2)%. The transit time in the RETPI beam is measured to be about 10 ms, and the ionization efficiency and the detection efficiency of MCP are estimated to be around 5%[45] and 50%,[46] respectively. Thus the number of trapped molecules in the $X^1\Sigma^+$ ($v'' = 0$) state is 48 (4), and the production rate of the $X^1\Sigma^+$ ($v'' = 0$) state molecules in ODT can be estimated to be 4800 (400) s^{-1}.

The time evolution of molecule number in the holding procedure can be described as[47]

$$\frac{dN_{mol}(t)}{dt} = -\Gamma_{BG}N_{mol}(t) - \frac{1}{\sqrt{(1+q_\alpha)^3}}\Gamma_{atom}N_{mol}(t) - \beta_H\int_V n^2(r,t)dr^3. \quad (4)$$

Here, Γ_{BG} is the loss rate of molecules due to their collision with the background gas, Γ_{atom} is the loss rate of inelastic co-trapped atom–molecule collisions, and β_H is the loss rate of molecule–molecule cold collisions. The factor $\sqrt{(1+q_\alpha)^3}$ takes into account of the different trap sizes for atoms and molecules, where q_α is the ratio between the atomic and molecular polarizabilities.[33] In the following analysis, the atomic polarizabilities are experimental values (^{85}Rb is 318.4 a.u.[48] and ^{133}Cs is 401.2 a.u.[49]). The molecular polarizability in the $X^1\Sigma^+$ ($v'' = 0$) state is 597.6 a.u., which is supported by explicit *ab initio* calculations.[50] As mentioned before, the β_H can be ignored. So eqn (4) is simplified as

$$\frac{dN_{mol}(t)}{dt} = -\left(\Gamma_{BG} + \frac{1}{\sqrt{(1+q_\alpha)^3}}\Gamma_{atom}\right)N_{mol}(t) = -\Gamma N_{mol}(t). \quad (5)$$

This equation can be solved as

$$N_{mol}(t) = N_0 e^{-t/\tau} \quad (6)$$

Here, τ is the typical lifetime and $\tau^{-1} = \Gamma$. The typical lifetime τ_{off} is 10 (5) ms and the molecules almost disappear after the release time, while τ_{on} is 19 (4) ms after the release time. Under "ODT off" conditions, the molecules are not trapped and surrounded by atoms prepared in dark-SPOTs, so the Γ_{off} comes from processes involving the molecule–background gas collisions, atom–molecule inelastic collisions and the dissipation process of thermal motion. Under "ODT on" conditions, the molecules have been confined in the ODT, and have longer lifetime. But, the molecular lifetime and number are still limited by the collisions, including the atom–molecule inelastic collisions.

To remove influences of atom–molecule inelastic collisions, pushing lasers are adopted in our experiment. By selectively turning on the pushing laser, the molecules or the molecules with chosen atoms could be prepared in ODT. Fig. 4(b) shows the time evolution of the $^{85}Rb^{133}Cs$ molecules, the molecules with ^{85}Rb atoms in the $F = 2$ state and ^{133}Cs atoms in the $F = 3$ state in the holding procedure. As we can see, the absence of cold atoms in the ODT significantly increases the number and lifetime of the trapped molecules.

The introduction of pushing lasers allows us to observe the atom–molecule collisions. In the molecular sample in the $X^1\Sigma^+$ ($v'' = 0$) state in the trap, the typical lifetime is 97 (20) ms, which is consistent with the background gas-limited lifetime for isolated ^{133}Cs atomic clouds in our measurement. These results also mean that the molecular lifetime is limited by collisions with the background gas. Under these conditions, $\Gamma_{atom} = 0$ and $\tau_1^{-1} = \Gamma_{BG} = 10$ (3) s^{-1} by fitting with eqn (6). So, the $\Gamma_{^{85}Rb}$ value is deduced to be 19 (4) s^{-1} from the data of molecules trapped with ^{85}Rb atoms, and the $\Gamma_{^{133}Cs}$ value is deduced to be 50 (12) s^{-1} from the data of molecules trapped with ^{133}Cs atoms. The sum of Γ_{RbCs}, $\Gamma_{^{85}Rb}$ and $\Gamma_{^{133}Cs}$ is 79 (8) s^{-1}, agreeing with the value of Γ_L. Γ_{atom} is related to the inelastic collision

rate K and $\Gamma_{atom} = Kn_{atom}$. Assuming that the atomic density is a constant, we extract $K_{^{85}Rb}$ as 1.0 (2) $\times 10^{-10}$ cm^3 s^{-1} and $K_{^{133}Cs}$ as 1.2 (3) $\times$ 10^{-10} cm^3 s^{-1} from our data. The released energy from the rovibrational quenching will remove the reactive atoms and molecules from the trap, thus the inelastic collisions of ^{85}Rb^{133}Cs molecules in the $X^1\Sigma^+$ ($v'' = 0$) state with ^{85}Rb (^{133}Cs) atoms are not affected by the inelastic collisions of ^{85}Rb^{133}Cs molecules in $X^1\Sigma^+$ ($v'' > 0$) states with ^{85}Rb (^{133}Cs) atoms. These values are on the same order as those reported in other experiments performed with trapped molecules in $a^3\Sigma^+$ states and the high lying level of $X^1\Sigma^+$ states, such as the ^{85}Rb^{133}Cs molecules in $a^3\Sigma^+$ states, ^{7}Li^{133}Cs molecules in $a^3\Sigma^+$ states and high lying level of $X^1\Sigma^+$ states.[31,33] Besides, our inelastic rate is still higher than the computed one,[33] which indicates that partial waves higher than the s-wave have to be involved in the collision under our experimental conditions. We notice that although the produced molecules populate in several vibrational states, the measured results should be the same as the case for pure $X^1\Sigma^+$ ($v'' = 0$) state ones, due to ignorable vibrational redistribution and molecule–molecule cold collisions.

Conclusion

We have shown that ultracold ^{85}Rb^{133}Cs molecules in the lowest vibrational $X^1\Sigma^+$ ($v'' = 0$) ground state (to be precise, the $J'' = 1$ and $J'' = 3$ states of $X^1\Sigma^+$ ($v'' = 0$)) produced *via* short-range PA have been confined in a crossed ODT. The loading and holding procedures of $X^1\Sigma^+$ ($v'' = 0$) state molecules in ODT are analyzed based on a phenomenological rate equation. The inelastic collisions of ^{85}Rb^{133}Cs molecules in the $X^1\Sigma^+$ ($v'' = 0$, $J'' = 1$ and $J'' = 3$) states with ultracold ^{85}Rb (or ^{133}Cs) atoms are measured. We note that ref. 51 has suggested that the $2^3\Pi_{0^+}$ state may have vibrational levels that permit efficient $X^1\Sigma^+$ ($v'' = 0$) state production in LiK, LiRb, LiCs, NaK, NaRb, NaCs and KCs systems. So, our demonstration provides a simple and generic procedure for studying the dynamical process of trapped cold molecules in singlet ground states.

Conflicts of interest

There are no conflicts to declare.

Acknowledgements

We thank Y. Hu, Y. Yang and C. Li for the meaningful discussions. The work was supported by the National Key Research and Development program (No. 2017YFA0304203), the National Natural Science Foundation of China (No. 61675120, 11434007 and 61378015), the NSFC Project for Excellent Research Team (No. 61121064), the Shanxi Scholarship Council of China, ''1331 KSC'', PCSIRT (No. IRT 13076), and the Applied Basic Research Project of Shanxi Province (No. 201601D202008).

References

1 M. Aymar and O. Dulieu, *J. Chem. Phys.*, 2005, **122**, 204302.
2 T. Zelevinsky, S. Kotochigova and J. Ye, *Phys. Rev. Lett.*, 2008, **100**, 043201.
3 S. Schiller, *Phys. Rev. Lett.*, 2007, **98**, 180801.
4 D. DeMille, S. B. Cahn, D. Murphree, D. A. Rahmlow and M. G. Kozlov, *Phys. Rev. Lett.*, 2008, **100**, 023003.
5 J. J. Gilijamse, S. Hoekstra, S. Y. T. van de Meerakker, G. C. Groenenboom and G. Meijer, *Science*, 2006, **313**, 1617.
6 S. Ospelkaus, K.-K. Ni, D. Wang, M. H. G. de Miranda, B. Neyenhuis, G. Quéméner, P. S. Julienne, J. L. Bohn, D. S. Jin and J. Ye, *Science*, 2010, **327**, 853.
7 D. DeMille, *Phys. Rev. Lett.*, 2002, **88**, 067901.
8 S. Ospelkaus, K.-K. Ni, G. Quéméner, B. Neyenhuis, D. Wang, M. H. G. de Miranda, J. L. Bohn, J. Ye and D. S. Jin, *Phys. Rev. Lett.*, 2010, **104**, 030402.
9 P. K. Molony, P. D. Gregory, Z. Ji, B. Lu, M. P. Köppinger, C. R. Le Sueur, C. L. Blackley, J. M. Hutson and S. L. Cornish, *Phys. Rev. Lett.*, 2014, **113**, 255301.
10 T. Takekoshi, L. Reichsöllner, A. Schindewolf, J. M. Hutson, C. R. Le Sueur, O. Dulieu, F. Ferlaino, R. Grimm and H.-C. Nägerl, *Phys. Rev. Lett.*, 2014, **113**, 205301.
11 J. W. Park, S. A. Will and M. W. Zwierlein, *Phys. Rev. Lett.*, 2015, **114**, 205302.
12 M. Guo, B. Zhu, B. Lu, X. Ye, F. Wang, R. Vexiau, N. Bouloufa-Maafa, G. Quéméner, O. Dulieu and D. Wang, *Phys. Rev. Lett.*, 2016, **116**, 205303.
13 J. M. Sage, S. Sainis, T. Bergeman and D. DeMille, *Phys. Rev. Lett.*, 2005, **94**, 203001.
14 K. Aikawa, D. Akamatsu, M. Hayashi, K. Oasa, J. Kobayashi, P. Naidon, T. Kishimoto, M. Ueda and S. Inouye, *Phys. Rev. Lett.*, 2010, **105**, 203001.
15 J. Banerjee, D. Rahmlow, R. Carollo, M. Bellos, E. E. Eyler, P. L. Gould and W. C. Stwalley, *Phys. Rev. A: At., Mol., Opt. Phys.*, 2012, **86**, 053428.
16 P. Zabawa, A. Wakim, M. Haruza and N. P. Bigelow, *Phys. Rev. A: At., Mol., Opt. Phys.*, 2011, **84**, 061401.
17 J. Deiglmayr, A. Grochola, M. Repp, K. Mörtlbauer, C. Glück, J. Lange, O. Dulieu, R. Wester and M. Weidemüller, *Phys. Rev. Lett.*, 2008, **101**, 133004.
18 C. D. Bruzewicz, M. Gustavsson, T. Shimasaki and D. DeMille, *New J. Phys.*, 2014, **16**, 023018.
19 I. C. Stevenson, D. B. Blasing, Y. P. Chen and D. S. Elliott, *Phys. Rev. A*, 2016, **94**, 062510.
20 M. Viteau, A. Chotia, M. Allegrini, N. Bouloufa, O. Dulieu, D. Comparat and P. Pillet, *Science*, 2008, **321**, 232.
21 I. Manai, R. Horchani, H. Lignier, P. Pillet, D. Comparat, A. Fioretti and M. Allegrini, *Phys. Rev. Lett.*, 2012, **109**, 183001.
22 C. Trefzger, C. Menotti and M. Lewenstein, *Phys. Rev. Lett.*, 2009, **103**, 035304.
23 M. Greiner, C. A. Regal and D. S. Jin, *Nature*, 2003, **426**, 537.
24 M. Bartenstein, A. Altmeyer, S. Riedl, S. Jochim, C. Chin, J. H. Denschlag and R. Grimm, *Phys. Rev. Lett.*, 2004, **92**, 120401.
25 H. L. Bethlem, G. Berden, F. M. H. Crompvoets, R. T. Jongma, A. J. A. van Roij and G. Meijer, *Nature*, 2000, **406**, 491.

26 B. Friedrich, J. D. Weinstein, R. deCarvalho and J. M. Doyle, *J. Chem. Phys.*, 1999, **110**, 2376.
27 S. C. Kuo and M. P. Sheetz, *Science*, 1993, **260**, 232.
28 N. Zahzam, T. Vogt, M. Mudrich, D. Comparat and P. Pillet, *Phys. Rev. Lett.*, 2006, **96**, 023202.
29 P. Staanum, S. D. Kraft, J. Lange, R. Wester and M. Weidemüller, *Phys. Rev. Lett.*, 2006, **96**, 023201.
30 C. Gabbanini, *Nucl. Phys. A*, 2007, **790**, 757c.
31 E. R. Hudson, N. B. Gilfoy, S. Kotochigova, J. M. Sage and D. DeMille, *Phys. Rev. Lett.*, 2008, **100**, 203201.
32 J. Deiglmayr, M. Repp, O. Dulieu, R. Wester and M. Weidemüller, *Eur. Phys. J. D*, 2011, **65**, 99.
33 J. Deiglmayr, M. Repp, R. Wester, O. Dulieu and M. Weidemuller, *Phys. Chem. Chem. Phys.*, 2011, **13**, 19101.
34 C. R. Menegatti, B. S. Marangoni and L. G. Marcassa, *Phys. Rev. A: At., Mol., Opt. Phys.*, 2011, **84**, 053405.
35 J.-R. Chen, C.-Y. Kao, H.-B. Chen and Y.-W. Liu, *New J. Phys.*, 2013, **15**, 043035.
36 H. Fahs, A. R. Allouche, M. Korek and M. Aubert-Frécon, *J. Phys. B: At., Mol. Opt. Phys.*, 2002, **35**, 1501.
37 C. Gabbanini and O. Dulieu, *Phys. Chem. Chem. Phys.*, 2011, **13**, 18905.
38 J. Yuan, Y. Zhao, Z. Ji, Z. Li, J.-T. Kim, L. Xiao and S. Jia, *J. Chem. Phys.*, 2015, **143**, 224312.
39 Y. Zhao, J. Yuan, Z. Ji, C. Li, Z. Li, L. Xiao and S. Jia, *J. Quant. Spectrosc. Radiat. Transfer*, 2016, **184**, 8.
40 T. Shimasaki, J.-T. Kim and D. DeMille, *Chem. Phys. Chem.*, 2016, **17**, 3677.
41 T. Shimasaki, M. Bellos, C. D. Bruzewicz, Z. Lasner and D. DeMille, *Phys. Rev. A: At., Mol., Opt. Phys.*, 2015, **91**, 021401.
42 W. Ketterle, K. B. Davis, M. A. Joffe, A. Martin and D. E. Pritchard, *Phys. Rev. Lett.*, 1993, **70**, 2253.
43 Y. Lee, Y. Yoon, S. Lee, J.-T. Kim and B. Kim, *J. Phys. Chem. A*, 2008, **112**, 7214.
44 S. J. M. Kuppens, K. L. Corwin, K. W. Miller, T. E. Chupp and C. E. Wieman, *Phys. Rev. A: At., Mol., Opt. Phys.*, 2000, **62**, 013406.
45 C. Drag, B. L. Tolra, O. Dulieu, D. Comparat, M. Vatasescu, S. Boussen, S. Guibal, A. Crubellier and P. Pillet, *IEEE J. Quantum Electron.*, 2000, **36**, 1378.
46 A. Altaf, S. Dutta, J. Lorenz, J. Prez-Ros, Y. P. Chen and D. S. Elliott, *J. Chem. Phys.*, 2015, **142**, 114310.
47 Although the trapped RbCs molecules populate in a series of vibrational distributions, the vibrational redistribution can be neglected as the lifetimes of RbCs in the lowest vibrational states are on the order of 10^4 s (see *J. Chem. Phys.*, 2004, **120**, 88 and *J. Chem. Phys.*, 2005, **123**, 174304), which are much larger than the measured lifetime of trapped molecules. The time evolutions of RbCs molecules in $X^1\Sigma^+$ ($v'' = 1$) and $X^1\Sigma^+$ ($v'' = 2$) states also express simple exponential decay functions with trapped lifetimes of 98 (15) ms and 96 (11) ms. These values are consistent with the $X^1\Sigma^+$ ($v'' = 0$) state, confirming the reasonability of neglecting vibrational redistribution. Furthermore, it is expected that the populations of molecules in the other vibrational states in the optical trap are the same as the dark-SPOTs in ref. 18.
48 R. W. Molof, H. L. Schwartz, T. M. Miller and B. Bederson, *Phys. Rev. A: At., Mol., Opt. Phys.*, 1974, **10**, 1131.
49 J. M. Amini and H. Gould, *Phys. Rev. Lett.*, 2003, **91**, 153001.
50 J. Deiglmayr, M. Aymar, R. Wester, M. Weidemüller and O. Dulieu, *J. Chem. Phys.*, 2008, **129**, 064309.
51 W. C. Stwalley, J. Banerjee, M. Bellos, R. Carollo, M. Recore and M. Mastroianni, *J. Phys. Chem. A*, 2010, **114**, 81.

